Non-linear Methods for Scalar Equations

Professor Dr. E F Toro

Laboratory of Applied Mathematics
University of Trento, Italy
eleuterio.toro@unitn.it
http://www.ing.unitn.it/toro

October 31, 2014

Abstract

- We construct non-linear second order methods for scalar equations, including source terms
- Two non-linear constraints are enforced: TVD and ENO
- Approaches: flux limiter methods and reconstruction methods
- Schemes derived: MUSCL-Hancock (one upwind and one centred), WAF and ADER

Flux Limiter Methods

We study a class of TVD schemes called flux limiter methods, as applied to

$$\partial_t q + \partial_x f(q) = 0 \ , \quad f(q) = \lambda q \ . \tag{1}$$

The schemes have conservative form

$$q_i^{n+1} = q_i^n - \frac{\Delta t}{\Delta x}\left(f_{i+\frac{1}{2}} - f_{i-\frac{1}{2}}\right) \tag{2}$$

with numerical flux

$$f_{i+\frac{1}{2}} = f_{i+\frac{1}{2}}^{LO} + \psi_{i+\frac{1}{2}}(f_{i+\frac{1}{2}}^{HO} - f_{i+\frac{1}{2}}^{LO}) \ . \tag{3}$$

$f_{i+\frac{1}{2}}^{LO}$: a monotone flux; $f_{i+\frac{1}{2}}^{HO}$: flux for second-order linear scheme. Here

$$\left.\begin{array}{l} f_{i+\frac{1}{2}}^{LO} = f_{i+\frac{1}{2}}^{GodU} = \left\{\begin{array}{ccc} \lambda q_i^n & \text{if} & \lambda > 0 \ , \\ \lambda q_{i+1}^n & \text{if} & \lambda < 0 \ , \end{array}\right. \\ \\ f_{i+\frac{1}{2}}^{HO} = f_{i+\frac{1}{2}}^{LW} = \frac{1}{2}(1+c)\lambda q_i^n + \frac{1}{2}(1-c)\lambda q_{i+1}^n \ . \end{array}\right\} \tag{4}$$

$\psi_{i+\frac{1}{2}}$ is called *flux limiter* and is constructed on TVD considerations.

We construct the TVD region, which is the range for the limiter function $\psi_{i+\frac{1}{2}}$. First we consider the case of positive characteristic speed, $\lambda > 0$.

Substitution of (4) into (3) gives

$$f_{i+\frac{1}{2}} = \lambda q_i^n + \frac{1}{2}(1-c)\lambda(q_{i+1}^n - q_i^n)\psi_{i+\frac{1}{2}} \ . \tag{5}$$

Inserting this flux into the conservative formula (2) gives

$$q_i^{n+1} = q_i^n - c[\Delta q_{i-\frac{1}{2}} + \frac{1}{2}(1-c)(\psi_{i+\frac{1}{2}}\Delta q_{i+\frac{1}{2}} - \psi_{i-\frac{1}{2}}\Delta q_{i-\frac{1}{2}})] \tag{6}$$

which if written in incremental form

$$q_i^{n+1} = q_i^n - C_{i-\frac{1}{2}}\Delta q_{i-\frac{1}{2}} + D_{i+\frac{1}{2}}\Delta q_{i+\frac{1}{2}} \tag{7}$$

has coefficients

$$C_{i-\frac{1}{2}} = c[1 - \frac{1}{2}(1-c)\psi_{i-\frac{1}{2}}] \ ; \ \ D_{i+\frac{1}{2}} = -\frac{1}{2}(1-c)c\psi_{i+\frac{1}{2}} \tag{8}$$

We note that (7) can be simplified by introducing the definition

$$r_{i+\frac{1}{2}} = \frac{\Delta q_{upw}}{\Delta q_{loc}} = \begin{cases} \dfrac{q_i^n - q_{i-1}^n}{q_{i+1}^n - q_i^n} & = & \dfrac{\Delta q_{i-\frac{1}{2}}}{\Delta q_{i+\frac{1}{2}}} & \text{if} \quad \lambda > 0 \,, \\ \\ \dfrac{q_{i+2}^n - q_{i+1}^n}{q_{i+1}^n - q_i^n} & = & \dfrac{\Delta q_{i+\frac{3}{2}}}{\Delta q_{i+\frac{1}{2}}} & \text{if} \quad \lambda < 0 \,. \end{cases} \tag{9}$$

Then for $\lambda > 0$ we have

$$\Delta q_{i+\frac{1}{2}} = \frac{\Delta q_{i-\frac{1}{2}}}{r_{i+\frac{1}{2}}} \,, \tag{10}$$

which if inserted in (7) gives

$$q_i^{n+1} = q_i^n - \hat{C}_{i-\frac{1}{2}} \Delta q_{i-\frac{1}{2}} + \hat{D}_{i+\frac{1}{2}} \Delta q_{i+\frac{1}{2}} \,, \tag{11}$$

with

$$\hat{C}_{i-\frac{1}{2}} = c\left(1 + \frac{1}{2}(1-c)\left(\frac{\psi_{i+\frac{1}{2}}}{r_{i+\frac{1}{2}}} - \psi_{i-\frac{1}{2}}\right)\right) \,, \;\; \hat{D}_{i+\frac{1}{2}} = 0 \,. \tag{12}$$

Recall that Harten's theorem requires

$$C_{i+\frac{1}{2}} \geq 0 \;, \quad D_{i+\frac{1}{2}} \geq 0 \;, \quad 0 \leq C_{i+\frac{1}{2}} + D_{i+\frac{1}{2}} \leq 1 \;. \tag{13}$$

For this to apply we simply need to enforce the following inequalities

$$0 \leq \hat{C}_{i-\frac{1}{2}} = c\left(1 + \frac{1}{2}(1-c)\left(\frac{\psi_{i+\frac{1}{2}}}{r_{i+\frac{1}{2}}} - \psi_{i-\frac{1}{2}}\right)\right) \leq 1 \;. \tag{14}$$

From now on we assume the following condition on the Courant number

$$0 \leq c \leq 1 \;. \tag{15}$$

Then, enforcing the left-hand side and the right-hand side of (14) leads to

$$-\frac{2}{1-c} \leq \frac{\psi_{i+\frac{1}{2}}}{r_{i+\frac{1}{2}}} - \psi_{i-\frac{1}{2}} \leq \frac{2}{c} \;. \tag{16}$$

We impose the following conditions on the limiter functions

$$0 \le \psi_{i-\frac{1}{2}} \le \frac{2}{1-c} \; , \;\; \forall i \; . \tag{17}$$

Then from (16) and (17) we can deduce the following pair of inequalities

$$-\frac{2}{1-c} \le \frac{\psi_{i+\frac{1}{2}}}{r_{i+\frac{1}{2}}} \le \frac{2}{c(1-c)} \; , \;\; \forall i \tag{18}$$

- Inequalities (17) give lower and upper bounds for the limiter functions.
- Inequalities (18) determine two inclined straight lines of slopes $-\frac{2}{1-c}$ and $\frac{2}{(1-c)c}$.
- The analysis for $\lambda < 0$ is analogous, so that c is replaced by $|c|$ in all equations. The resulting general TVD region in the r-ψ plane is depicted in Fig. 1.

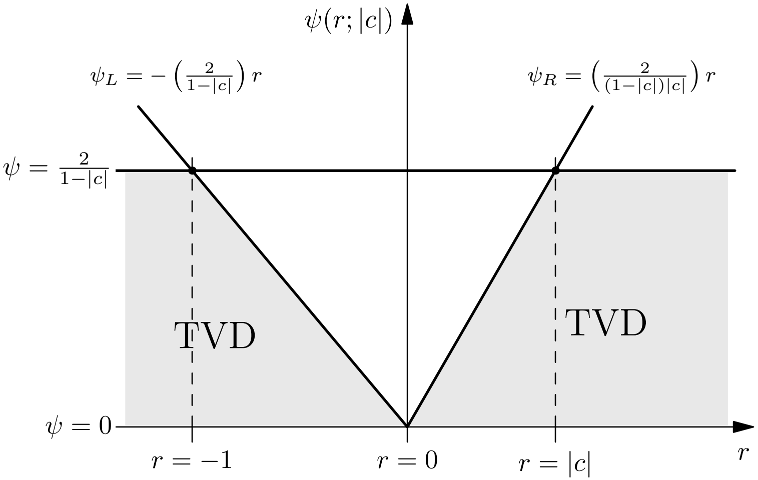

Fig. 1: General TVD region for the flux limiter method based on the Godunov upwind and Lax-Wendroff methods.

The complete general TVD region is given by

$$0 \leq \psi_{i+\frac{1}{2}} \leq \psi_{max}(r) \ , \ \ \forall i \ , \tag{19}$$

with

$$\psi_{max}(r) = \begin{cases} \text{Negative r} \begin{cases} \dfrac{2}{1-|c|} & \text{if} \quad r \leq -1 \ , \\ -\dfrac{2}{(1-|c|)} r & \text{if} \quad -1 \leq r \leq 0 \ , \end{cases} \\ \text{Positive r} \begin{cases} \dfrac{2}{(1-|c|)|c|} r & \text{if} \quad 0 \leq r \leq |c| \ , \\ \dfrac{2}{1-|c|} & \text{if} \quad r \geq |c| \ . \end{cases} \end{cases} \tag{20}$$

The Sweby TVD region [10] is a subset of the general TVD region derived above and is obtained by defining

$$\psi_{max}^{Sweby}(r) = \begin{cases} 0 \quad \text{if} \quad r \leq 0\,, \\ \begin{cases} \dfrac{2}{r} \quad \text{if} \quad 0 \leq r \leq \dfrac{1}{2}\,, \\ 2 \quad \text{if} \quad r \geq \dfrac{1}{2} \end{cases} \end{cases} \tag{21}$$

in (19).

- The Sweby TVD region is depicted by the shaded zone of Fig. 2, to the right of $\psi = 2r$, above $\psi = 0$ and below $\psi = 2$; also, $\psi = 0$ for $r \leq 0$ is part of the TVD region.
- Any function $\psi(r)$ within this region, called a *flux limiter*, produces a TVD scheme
- Not every choice produces a *good* TVD scheme.

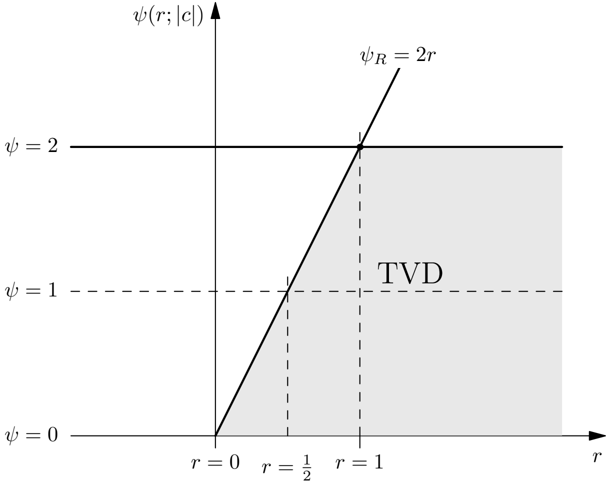

Fig. 2: Sweby's TVD region for the flux limiter method based on the Godunov upwind and the Lax-Wendroff methods.

Limiter functions

Popular choices for flux limiters are the SUPERBEE limiter

$$\psi_{sb}(r) = \begin{cases} 0 & \text{if} \quad r \leq 0\,, \\ 2r & \text{if} \quad 0 \leq r \leq \frac{1}{2}\,, \\ 1 & \text{if} \quad \frac{1}{2} \leq r \leq 1\,, \\ r & \text{if} \quad 1 \leq r \leq 2\,, \\ 2 & \text{if} \quad r \geq 2\,, \end{cases} \tag{22}$$

the VANLEER limiter

$$\psi_{vl}(r) = \begin{cases} 0 & \text{if} \quad r \leq 0\,, \\ \dfrac{2r}{1+r} & \text{if} \quad r \geq 0\,, \end{cases} \tag{23}$$

the VANALBADA limiter

$$\psi_{va}(r) = \begin{cases} 0 & \text{if} \quad r \leq 0 \, , \\ \dfrac{r(1+r)}{1+r^2} & \text{if} \quad r \geq 0 \, , \end{cases} \tag{24}$$

and the MINBEE (or MINMOD) limiter

$$\psi_{mb}(r) = \begin{cases} 0 & \text{if} \quad r \leq 0 \, , \\ r & \text{if} \quad 0 \leq r \leq 1 \, , \\ 1 & \text{if} \quad r \geq 1 \, . \end{cases} \tag{25}$$

The WAF method

The WAF method (Weighted Average Flux) is a conservative method

$$q_i^{n+1} = q_i^n - \frac{\Delta t}{\Delta x}\left(f_{i+\frac{1}{2}} - f_{i-\frac{1}{2}}\right) \; , \tag{26}$$

with numerical flux

$$f_{i+\frac{1}{2}}^{waf} = \frac{1}{\Delta x}\int_{-\frac{1}{2}\Delta x}^{\frac{1}{2}\Delta x} f(q_{i+\frac{1}{2}}(x, \frac{1}{2}\Delta t))dx \; . \tag{27}$$

See Toro (1989) [11].

- The integration range in (27) goes from the middle of cell I_i (left of the interface) to the middle of cell I_{i+1} (right of the interface)
- The integrand is the physical flux function $f(q)$ in the conservation law
- $q_{i+\frac{1}{2}}(x, \frac{1}{2}\Delta t)$ is the solution of the classical Riemann problem with data $(q_i^n$ (left) and $q_{i+1}^n)$ (right)
- The flux formula can be generalised in a number of ways, to include for example, irregular meshes

WAF applied to the linear advection equation

For the linear advection equation the classical Riemann problem is

$$\left.\begin{array}{ll} \text{PDE:} & \partial_t q(x,t) + \partial_x f(q(x,t)) = 0 \;, \quad f(q(x,t)) = \lambda q(x,t) \;, \\ \text{IC:} & q(x,0) = \begin{cases} q_i^n & \text{if} \quad x < 0 \;, \\ q_{i+1}^n & \text{if} \quad x > 0 \;. \end{cases} \end{array}\right\} \tag{28}$$

The solution is

$$q_{i+\frac{1}{2}}(x,t) = \begin{cases} q_i^n & \text{if} \quad \dfrac{x}{t} < \lambda \;, \\ \\ q_{i+1}^n & \text{if} \quad \dfrac{x}{t} > \lambda \;. \end{cases} \tag{29}$$

Simple calculations show that the WAF flux is

$$f_{i+\frac{1}{2}}^{waf} = \frac{1}{2}(1+c)(\lambda q_i^n) + \frac{1}{2}(1-c)(\lambda q_{i+1}^n) \;. \tag{30}$$

See Fig. 3.

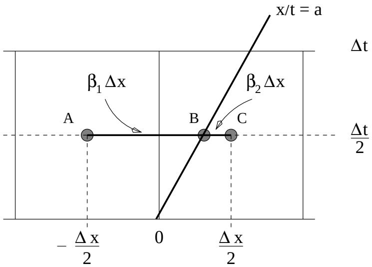

Fig. 3: The WAF flux for the linear advection equation, for $\lambda > 0$.

- The WAF flux is identical to the Lax-Wendroff flux. This is only true for the linear advection equation. For non-linear equations WAF is a Riemann-problem based generalisation of the Lax-Wendroff method
- The flux is a weighted average of the upwind weight $\frac{1}{2}(1 + c)$ and the downwind weight $\frac{1}{2}(1 - c)$
- The upwind weight controls monotonicity and the downwind weight controls accuracy
- A TVD version will reduce the downwind contribution, when necessary, in favour of the upwind weight

TVD version of WAF

First note that the WAF flux can be written as

$$f_{i+\frac{1}{2}}^{waf} = \frac{1}{2}(\lambda q_i^n + \lambda q_{i+1}^n) - \frac{1}{2}c(q_{i+1}^n - q_i^n)\ . \tag{31}$$

The TVD version is

$$f_{i+\frac{1}{2}}^{waf} = \frac{1}{2}(\lambda q_i^n + \lambda q_{i+1}^n) - \frac{1}{2}\text{sign (c)}\psi_{i+\frac{1}{2}}^{waflim}(\lambda q_{i+1}^n - \lambda q_i^n)\ . \tag{32}$$

Here

$$\psi_{i+\frac{1}{2}}^{waflim} = 1 - (1 - |c|)\psi_{i+\frac{1}{2}}^{fluxlim} \tag{33}$$

where $\psi_{i+\frac{1}{2}}^{fluxlim}$ is a flux limiter function. This version of the scheme circumvents Godunov's theorem: the resulting scheme is non-linear.
For complete details on the WAF method and the construction of its TVD version see Chapter 13 of Toro (2009) [12].

Reconstruction-based Methods

Recall that cell averages are

$$q_i^n \approx \frac{1}{\Delta x} \int_{x_{i-\frac{1}{2}}}^{x_{i+\frac{1}{2}}} q(x, t_n) dx \ , \tag{34}$$

within the cell $[x_{i-\frac{1}{2}}, x_{i+\frac{1}{2}}]$, at time $t = t_n$.

Given a set of cell averages $\{q_i^n\}$ at time level n we construct polynomials $p_i(x)$, see Fig. 4, such that they satisfy:

1. *The conservation property*. One expects the integral averages of the reconstructed functions to coincide with the original averages, that is

$$q_i^n = \frac{1}{\Delta x} \int_{x_{i-\frac{1}{2}}}^{x_{i+\frac{1}{2}}} p_i(x) dx \ . \tag{35}$$

2. *The non-oscillatory property*. To this end one imposes a TVD condition or an *Essentially Non-Oscillatory* (ENO) property, for example. This part of the scheme circumvents Godunov's theorem by constructing a non-linear scheme.

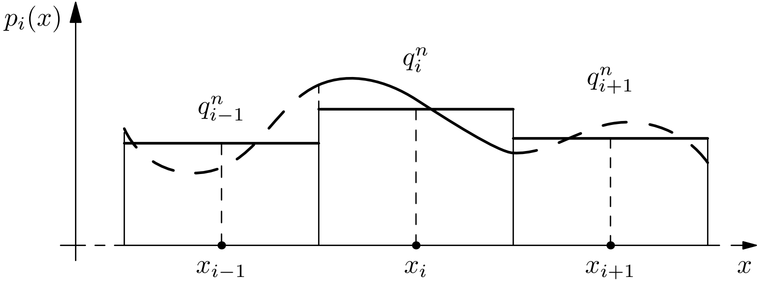

Fig. 4. Reconstruction polynomial function $p_i(x)$ from cell averages $\{q_j^n\}$.

We study the simplest case, first-degree polynomials of the form

$$p_i(x) = q_i^n + (x - x_i)\Delta_i \tag{36}$$

within the cell $[x_{i-\frac{1}{2}}, x_{i+\frac{1}{2}}]$, at time $t = t_n$. Here $x_i = \frac{1}{2}(x_{i-\frac{1}{2}} + x_{i+\frac{1}{2}})$ is the cell centre and Δ_i is the slope of $p_i(x)$, still to be determined.
Fig. 5 depicts two polynomials of the form (36) and are determined by respectively choosing the slopes

$$\Delta_i \equiv \Delta_{i-\frac{1}{2}} = \frac{q_i^n - q_{i-1}^n}{\Delta x}\ , \ \ \Delta_i \equiv \Delta_{i+\frac{1}{2}} = \frac{q_{i+1}^n - q_i^n}{\Delta x}\ . \tag{37}$$

TVD slopes

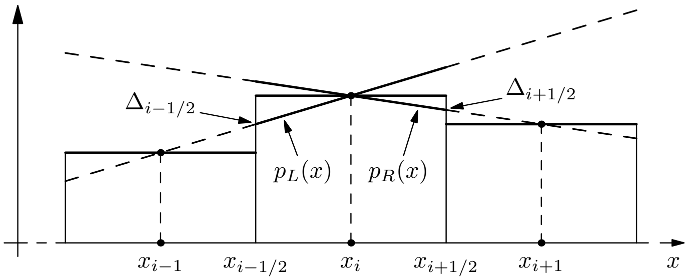

Fig. 5. Reconstruction functions $p_L(x)$, $p_R(x)$ from q^n_{i-1}, q^n_i, q^n_{i+1}.

The minmod slope. This has the following form

$$\Delta_i = minmod(\Delta_{i-\frac{1}{2}}, \Delta_{i+\frac{1}{2}}) \ , \tag{38}$$

where the minmod function is defined as

$$minmod(x, y) = \begin{cases} x & \text{if} \quad |x| \le |y| \text{ and } xy > 0 \ , \\ y & \text{if} \quad |x| > |y| \text{ and } xy > 0 \ , \\ 0 & \text{if} \quad xy < 0 \ . \end{cases} \tag{39}$$

The superbee slope. This has the following form

$$\Delta_i = maxmod(\Delta_i^{(1)}, \Delta_i^{(2)}) \ , \tag{40}$$

where

$$\Delta_i^{(1)} = minmod(\Delta_{i+\frac{1}{2}}, 2\Delta_{i-\frac{1}{2}}) \ , \ \ \Delta_i^{(2)} = minmod(2\Delta_{i+\frac{1}{2}}, \Delta_{i-\frac{1}{2}}) \tag{41}$$

and

$$maxmod(x,y) = \begin{cases} x & \text{if} \quad |x| \geq |y| \text{ and } xy > 0 \ , \\ y & \text{if} \quad |x| \leq |y| \text{ and } xy > 0 \ , \\ 0 & \text{if} \quad xy < 0 \ . \end{cases} \tag{42}$$

The MC slope. This has the following form

$$\Delta_i = minmod(\Delta_i^{(c)}, 2\Delta_{i-\frac{1}{2}}, 2\Delta_{i+\frac{1}{2}}) \ , \tag{43}$$

where

$$\Delta_i^{(c)} = \frac{1}{2}(\Delta_{i-\frac{1}{2}} + \Delta_{i+\frac{1}{2}}) \ . \tag{44}$$

is the *centred* slope.

ENO reconstruction

- ENO (Essentially Non-Oscillatory) approach due to Harten et al. (1987) [5] is used for reconstructions that satisfy the conservation and the non-oscillatory properties.
- In ENO the choice of slope Δ_i is made by analysing two potential candidate stencils S_L and S_R and their corresponding polynomials $p_L(x)$ and $p_R(x)$, namely

$$\left.\begin{array}{lll} \text{Left stencil:} & S_L = \{i-1, i\} \quad \rightarrow & p_L(x) = a_L + b_L x \;, \\ \text{Right stencil:} & S_R = \{i, i+1\} \quad \rightarrow & p_R(x) = a_R + b_R x \;. \end{array}\right\} \quad (45)$$

The coefficients a_L, b_L, a_R and b_R are to be found. See Fig. 5.

- Each candidate polynomial for each stencil must satisfy the conservation property, for each cell in the stencil.
- For the left stencil S_L the conservation property requires

$$\frac{1}{\Delta x}\int_{x_{i-\frac{3}{2}}}^{x_{i-\frac{1}{2}}} p_L(x)dx = q_{i-1}^n \;, \quad \frac{1}{\Delta x}\int_{x_{i-\frac{1}{2}}}^{x_{i+\frac{1}{2}}} p_L(x)dx = q_i^n \;. \quad (46)$$

On exact integration one obtains

$$\Delta_i \equiv \Delta_{i-\frac{1}{2}} = \frac{q_i^n - q_{i-1}^n}{\Delta x} \; . \tag{47}$$

Similarly, by imposing conservation on the polynomial $p_R(x)$ based on the right stencil S_R we have

$$\frac{1}{\Delta x}\int_{x_{i-\frac{1}{2}}}^{x_{i+\frac{1}{2}}} p_R(x)dx = q_i^n \; , \quad \frac{1}{\Delta x}\int_{x_{i+\frac{1}{2}}}^{x_{i+\frac{3}{2}}} p_R(x)dx = q_{i+1}^n \; . \tag{48}$$

After exact integration we obtain

$$\Delta_i \equiv \Delta_{i+\frac{1}{2}} = \frac{q_{i+1}^n - q_i^n}{\Delta x} \; . \tag{49}$$

Then the resulting two possible choices for the reconstruction polynomial are

$$p_i(x) = \begin{cases} p_L(x) = q_i^n + (x - x_i)\left(\dfrac{q_i^n - q_{i-1}^n}{\Delta x}\right) \; , \\ \\ p_R(x) = q_i^n + (x - x_i)\left(\dfrac{q_{i+1}^n - q_i^n}{\Delta x}\right) \; . \end{cases} \tag{50}$$

The ENO method selects the polynomial with the smallest slope in absolute value, namely

$$\Delta_i^{ENO} = \begin{cases} \Delta_{i-\frac{1}{2}} & \text{if} \quad |\Delta_{i-\frac{1}{2}}| \leq |\Delta_{i+\frac{1}{2}}| \,, \\ \\ \Delta_{i+\frac{1}{2}} & \text{if} \quad |\Delta_{i-\frac{1}{2}}| > |\Delta_{i+\frac{1}{2}}| \,. \end{cases} \tag{51}$$

Thus the resulting ENO polynomial is

$$p_i^{ENO}(x) = \begin{cases} p_L(x) = q_i^n + (x - x_i)\left(\dfrac{q_i^n - q_{i-1}^n}{\Delta x}\right) & \text{if } |\Delta_{i-\frac{1}{2}}| \leq |\Delta_{i+\frac{1}{2}}|; \\ \\ p_R(x) = q_i^n + (x - x_i)\left(\dfrac{q_{i+1}^n - q_i^n}{\Delta x}\right) & \text{if } |\Delta_{i-\frac{1}{2}}| > |\Delta_{i+\frac{1}{2}}| \end{cases} \tag{52}$$

Compare the ENO slope (51) with the minmod TVD slope (38).

Remarks on reconstruction schemes

1. A modification of the ENO approach, called WENO (for weighted ENO), uses all candidate stencils in the ENO approach to produce the WENO polynomial, which is a linear combination of all candidate ENO polynomials. See the work of Jiang and Shu (1996) [6].

2. An ENO reconstruction is not TVD an the resulting ENO numerical scheme admits spurious oscillations with new extrema. However, on mesh refinement the amplitude of the spurious oscillations tends to zero as the mesh width tends to zero. This property is not satisfied by linear schemes.

3. The ENO and WENO reconstruction approaches can be extended to any order of accuracy in one, two and three space dimensions. See [3], [4] on recent advances on reconstruction procedures in multiple space dimensions.

The MUSCL-Hancock scheme

To compute the numerical flux $f_{i+\frac{1}{2}}$ one performs the following four steps:

- *Step (I): Reconstruction.* Use polynomial (36). See Fig. 6.

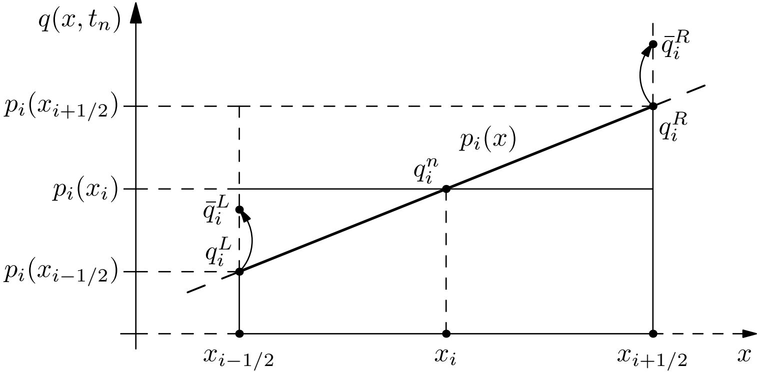

Fig. 6. MUSCL-Hancock scheme. The reconstructed 1st-degree polynomial $p_i(x)$ has boundary extrapolated values q_i^L (left) and q_i^R (right). These are then evolved in time to become $\overline{q}_i^L$ and $\overline{q}_i^R$.

- *Step (II): Cell-boundary values*, or *boundary extrapolated values*

$$q_i^L = p_i(x_{i-\frac{1}{2}}) = q_i^n - \frac{1}{2}\Delta x \Delta_i \; ; \quad q_i^R = p_i(x_{i+\frac{1}{2}}) = q_i^n + \frac{1}{2}\Delta x \Delta_i \; . \tag{53}$$

- *Step (III): Evolution of cell-boundary values* for a time $\frac{1}{2}\Delta t$

$$\left.\begin{aligned} \overline{q}_i^L &= q_i^L - \frac{1}{2}\frac{\Delta t}{\Delta x}[f(q_i^R) - f(q_i^L)] = q_i^n - \frac{1}{2}(1+c)\Delta x \Delta_i \; , \\ \overline{q}_i^R &= q_i^R - \frac{1}{2}\frac{\Delta t}{\Delta x}[f(q_i^R) - f(q_i^L)] = q_i^n + \frac{1}{2}(1-c)\Delta x \Delta_i \; . \end{aligned}\right\} \tag{54}$$

See Fig. 6.

- *Step (IV): The Riemann problem.* To compute $f_{i+\frac{1}{2}}$ one solves the *classical* Riemann problem. For the linear advection equation this is:

$$\left.\begin{aligned} &\text{PDE:} \qquad \partial_t q + \partial_x(\lambda q) = 0 \; , \\ &\text{IC:} \qquad q(x,0) = \begin{cases} \overline{q}_i^R = q_i^n + \frac{1}{2}(1-c)\Delta x \Delta_i & \text{if } x < 0 \; , \\ \overline{q}_{i+1}^L = q_{i+1}^n - \frac{1}{2}(1+c)\Delta x \Delta_{i+1} & \text{if } x > 0 \; . \end{cases} \end{aligned}\right\} \tag{55}$$

See Fig. 7 for al illustration of the Riemann problem with evolved initial conditions.

The similarity solution $q_{i+\frac{1}{2}}(x/t)$ is

$$q_{i+\frac{1}{2}}(x/t) = \begin{cases} \overline{q}_i^R = q_i^n + \frac{1}{2}(1-c)\Delta x \Delta_i & \text{if} \quad x/t < \lambda \, , \\ \\ \overline{q}_{i+1}^L = q_{i+1}^n - \frac{1}{2}(1+c)\Delta x \Delta_{i+1} & \text{if} \quad x/t > \lambda \, . \end{cases}$$

and the flux is

$$f_{i+\frac{1}{2}} = f(q_{i+\frac{1}{2}}(0)) = \begin{cases} \lambda \overline{q}_i^R = \lambda \left(q_i^n + \frac{1}{2}(1-c)\Delta x \Delta_i \right) & \text{if } \lambda > 0 \, , \\ \\ \lambda \overline{q}_{i+1}^L = \lambda \left(q_{i+1}^n - \frac{1}{2}(1+c)\Delta x \Delta_{i+1} \right) & \text{if } \lambda < 0 \, . \end{cases} \tag{56}$$

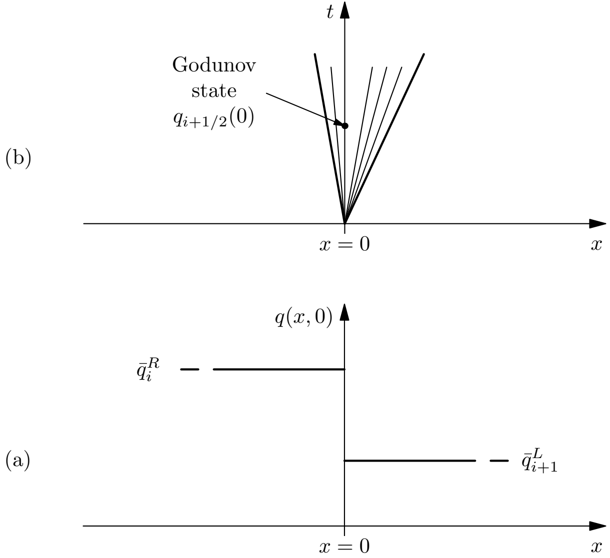

Fig. 7. Step IV of the MUSCL-Hancock method. (a) shows the the piece-wise constant data for the classical Riemann problem obtained from the evolved extrapolated values. (b) illustrates the similarity solution of the Riemann problem and the Godunov state right at the interface, along the t axis.

Well-known, linear second-order methods can be reproduced, in particular:

$$\Delta_i = \begin{cases} \Delta_{i-\frac{1}{2}} & = & \dfrac{q_i^n - q_{i-1}^n}{\Delta x} & (\text{ Warming-Beam }) \quad \lambda > 0 \; , \\ \Delta_{i+\frac{1}{2}} & = & \dfrac{q_{i+1}^n - q_i^n}{\Delta x} & (\text{ Lax-Wendroff }) \quad \lambda > 0 \; , \\ \Delta_c & = & \dfrac{q_{i+1}^n - q_{i-1}^n}{2\Delta x} & (\text{ Fromm}) \; . \end{cases} \tag{57}$$

- These schemes are linear, of second-order accuracy and produce spurious oscillations with new extrema
- In order to avoid or control the spurious oscillations in a MUSCL-Hancock type scheme we must select the slopes in a nonlinear manner, as discussed previously

FORCE-based variant of MUSCL-Hancock

- Instead of solving the Riemann problem in step (IV), see Fig. 7, for the MUSCL-Hancock scheme and computing the Godunov flux, one can use a simple, monotone numerical flux, such as the FORCE flux:

$$f_{i+\frac{1}{2}}^{force} = f_{i+\frac{1}{2}}^{force}(r,s)\ ,\ \ r = \overline{q}_i^R\ ,\ \ s = \overline{q}_{i+1}^L\ . \qquad (58)$$

- For the linear advection equation the FORCE flux is given as

$$f_{i+\frac{1}{2}}^{force}(r,s) = \frac{(1+c)^2}{4c}(\lambda r) - \frac{(1-c)^2}{4c}(\lambda s)\ . \qquad (59)$$

- This approach is applicable to general non-linear systems and the resulting schemes are simple and effective, though not as accurate as Riemann-problem based schemes, particularly for certain types or problems involving slowly moving intermediate waves.

Recalling the finite volume framework

Consider the general balance law

$$\partial_t q + \partial_x f(q) = s(q) \; . \tag{60}$$

Integrate (60) on finite volume $[x_{i-\frac{1}{2}}, x_{i+\frac{1}{2}}] \times [t_n, t_{n+1}]$ to obtain

$$q_i^{n+1} = q_i^n - \frac{\Delta t}{\Delta x}[f_{i+\frac{1}{2}} - f_{i-\frac{1}{2}}] + \Delta t s_i \; , \tag{61}$$

where

$$\left.\begin{array}{lcl} q_i^n & = & \frac{1}{\Delta x}\int_{x_{i-\frac{1}{2}}}^{x_{i+\frac{1}{2}}} q(x, t_n) dx \; , \\ f_{i+\frac{1}{2}} & = & \frac{1}{\Delta t}\int_{t_n}^{t_{n+1}} f(q(x_{i+\frac{1}{2}}, t)) dt \; , \\ s_i & = & \frac{1}{\Delta t}\frac{1}{\Delta x}\int_{t_n}^{t_{n+1}}\int_{x_{i-\frac{1}{2}}}^{x_{i+\frac{1}{2}}} s(q(x,t)) dx dt \; , \end{array}\right\} \tag{62}$$

with

$$\Delta x = x_{i+\frac{1}{2}} - x_{i-\frac{1}{2}} \; , \quad \Delta t = t_{n+1} - t_n \; , \quad x_i = \frac{1}{2}(x_{i-\frac{1}{2}} + x_{i+\frac{1}{2}}) \; . \tag{63}$$

- Formula (61) is the starting point for constructing *finite volume methods*
- This is achieved by constructing approximations to the integrals in (62), resulting in the, approximate, *finite volume formula*:

$$\hat{q}_i^{n+1} = \hat{q}_i^n - \frac{\Delta t}{\Delta x}[\hat{f}_{i+\frac{1}{2}} - \hat{f}_{i-\frac{1}{2}}] + \Delta t \hat{s}_i \ . \tag{64}$$

- This formula is used to evolve, in time, approximations to the cells averages in (62)
- In order to fully determine a finite volume formula (64) one requires:
  - $\hat{f}_{i+\frac{1}{2}}$: **the numerical flux**, an approximation to $f_{i+\frac{1}{2}}$ in (61)
  - $\hat{s}_i$: **the numerical source**, an approximation to s_i in (61)
- Often one refers directly to (61) as the finite volume scheme, but (64) is the correct interpretation.
- The accuracy of the resulting numerical scheme depends crucially on the accuracy used to approximate the integrals in (62)

The ADER Approach

ADER, first suggested by Toro et al. (2001) [13], is an approach for constructing non-linear numerical schemes of arbitrary order of accuracy in both space and time. Here we restrict the presentation to second order as applied to the linear advection equation. ADER has the following stages:

Step (A): Reconstruction. The simplest case is

$$p_i(x) = q_i^n + \Delta_i(x - x_i) \ , \ \ p_{i+1}(x) = q_{i+1}^n + \Delta_{i+1}(x - x_{i+1}) \ . \qquad (65)$$

Step (B): Generalized Riemann problem. For the linear advection equation with linear source term, the simplest case, denoted by GRP_1, is

$$\left.\begin{array}{rl} \text{PDE:} & \partial_t q + \lambda \partial_x q = \beta q \ , \\ \text{IC:} & q(x,0) = \left\{ \begin{array}{lll} p_i(x) & \text{if} & x < 0 \ , \\ p_{i+1}(x) & \text{if} & x > 0 \ , \end{array} \right. \end{array} \right\} \qquad (66)$$

whose solution is used to find the numerical flux $\hat{f}_{i+\frac{1}{2}}$ according to (62).

Step C: Numerical source. One requires an approximation $\hat{s}_i$ to the volume integral in (62) to find the numerical source.

Step (B): generalised Riemann problem and the numerical flux

We express the solution $q_{i+\frac{1}{2}}(\tau)$ as a truncated power series expansion

$$q_{i+\frac{1}{2}}(\tau) = q(0, 0_+) + \tau \partial_t q(0, 0_+) \ . \tag{67}$$

B1: The leading term $q(0, 0_+)$. One solves the classical Riemann problem

$$\left.\begin{array}{ll} \text{PDE:} & \partial_t q + \lambda \partial_x q = 0 \ , \\ & \\ \text{IC:} & q(x,0) = \begin{cases} p_i(0) \equiv \quad q_i^n + \frac{1}{2}\Delta x \Delta_i & \text{if } x < 0 \ , \\ p_{i+1}(0) \equiv \quad q_{i+1}^n - \frac{1}{2}\Delta x \Delta_{i+1} & \text{if } x > 0 \ , \end{cases} \end{array}\right\} \tag{68}$$

The similarity $d^{(0)}_{i+\frac{1}{2}}(x/t)$ of this problem is

$$d^{(0)}_{i+\frac{1}{2}}(x/t) = \begin{cases} q_i^n + \frac{1}{2}\Delta x \Delta_i & \text{if} \quad x/t < \lambda \ , \\ & \\ q_{i+1}^n - \frac{1}{2}\Delta x \Delta_{i+1} & \text{if} \quad x/t > \lambda \ . \end{cases} \tag{69}$$

The leading term in (67) is called *the Godunov state*; it is the solution (69) along the interface $x/t = 0$, that is

$$q(0, 0_+) = d^{(0)}_{i+\frac{1}{2}}(0) = \begin{cases} q_i^n + \frac{1}{2}\Delta x \Delta_i & \text{if} \quad \lambda > 0 \ , \\ \\ q_{i+1}^n - \frac{1}{2}\Delta x \Delta_{i+1} & \text{if} \quad \lambda < 0 \ . \end{cases} \tag{70}$$

Remark: Upto this point we have the **Kolgan scheme** (Kolgan, 1972) [7], whose linear version is however unstable.

The reader is encouraged to derive the Kolgan scheme and analyse its linear stability.

Note: Kolgan is credited to have been the first researcher to have constructed a non-linear scheme (1972), a scheme that circumvents Godunov's theorem. See [8] for a English translation of the original Russian article.

B2: The higher order term. To compute the second term in (67) we do the following:

- *Time derivative in terms of the spatial derivative.* We apply the Cauchy-Kowalewski procedure whereby the PDE in (68) is used to express the time derivative in terms of the space derivative and the source term, that is

$$\partial_t q(x,t) = -\lambda \partial_x q(x,t) + \beta q(x,t) \; . \tag{71}$$

  The sought term $\partial_t q(x,t)$ will be known once the source function $\beta q(x,t)$ and the spatial gradient $\partial_x q(x,t)$ are known. These are required at the leading term, so that the expansion (67) reads

$$q_{i+\frac{1}{2}}(\tau) = q(0,0_+) + [-\lambda \partial_x q(0,0_+) + \beta q(0,0_+)]\tau \; . \tag{72}$$

  The gradient $\partial_x q(0,0_+)$ remains unknown.

- *Evolution equation for the space derivative.*

$$\partial_t(\partial_x q(x,t)) + \lambda \partial_x(\partial_x q(x,t)) = \beta \partial_x q(x,t) \; . \tag{73}$$

- *Riemann problem for the spatial derivative.* We simplify (73) by neglecting the source term for the gradient. For the model equation this can be justified.
- Then we pose the classical homogeneous Riemann problem for the spatial derivative, namely

$$\left.\begin{array}{ll} \text{PDE:} & \partial_t(\partial_x q(x,t)) + \lambda \partial_x(\partial_x q(x,t)) = 0 \; , \\ \text{IC:} & \partial_x q(x,0) = \left\{ \begin{array}{lll} \Delta_i & \text{if} & x < 0 \; , \\ \Delta_{i+1} & \text{if} & x > 0 \; . \end{array} \right. \end{array} \right\} \tag{74}$$

We solve the classical Riemann problem (74)

$$d^{(1)}_{i+\frac{1}{2}}(x/t) = \begin{cases} \Delta_i & \text{if} \quad x/t < \lambda \ , \\ \\ \Delta_{i+1} & \text{if} \quad x/t > \lambda \ . \end{cases} \tag{75}$$

We need the Godunov state at $x/t = 0$ at the interface, which is

$$\partial_x q(0, 0_+) = d^{(1)}_{i+\frac{1}{2}}(0) = \begin{cases} \Delta_i & \text{if} \quad \lambda > 0 \ , \\ \\ \Delta_{i+1} & \text{if} \quad \lambda < 0 \end{cases} \tag{76}$$

The sought solution (67) is

$$q_{i+\frac{1}{2}}(\tau) =$$

$$\begin{cases} q_i^n + \frac{1}{2}\Delta x \Delta_i + \tau \left[-\lambda \Delta_i + \beta(q_i^n + \frac{1}{2}\Delta x \Delta_i) \right] \ , & \lambda > 0 \ , \\ \\ q_{i+1}^n - \frac{1}{2}\Delta x \Delta_{i+1}) + \tau \left[-\lambda \Delta_{i+1} + \beta(q_{i+1}^n - \frac{1}{2}\Delta x \Delta_{i+1}) \right] \ , & \lambda < 0 \ . \end{cases} \tag{77}$$

The numerical flux in (61) is obtained according to (62), namely

$$f_{i+\frac{1}{2}} \frac{1}{\Delta t} \int_{t_n}^{t_{n+1}} f(q_{i+\frac{1}{2}}(\tau)) d\tau \ . \tag{78}$$

By performing exact integration one obtains

$$f_{i+\frac{1}{2}} = \begin{cases} \lambda \left(q_i^n + \frac{1}{2}(1-c)\Delta x \Delta_i + \frac{1}{2} r (q_i^n + \frac{1}{2}\Delta x \Delta_i) \right) & , \ \lambda > 0 \\ \\ \lambda \left(q_{i+1}^n - \frac{1}{2}(1+c)\Delta x \Delta_{i+1}) + \frac{1}{2} r (q_{i+1}^n - \frac{1}{2}\Delta x \Delta_{i+1}) \right) & , \ \lambda < 0 \end{cases} \tag{79}$$

where $c = \lambda \Delta t / \Delta x$ is the Courant number and $r = \Delta t \beta$ is a dimensionless *reaction* number.

- The ADER numerical flux (79) includes a contribution due to the source term. In other words, the flux knows of the source term, as one would expect.
- But note that there is still another contribution to the scheme resulting from the *numerical source*, still to be specified.

Step (C): numerical source

- The numerical source in (61) is obtained according to (62), namely

$$s_i = \frac{1}{\Delta t}\frac{1}{\Delta x}\int_{t_n}^{t_{n+1}}\int_{x_{i-\frac{1}{2}}}^{x_{i+\frac{1}{2}}} s(q_i(x,t))dxdt \; . \tag{80}$$

  $q_i(x,t)$ is an approximation in the control volume. To second-order, the mid-point integration rule suffices, and one requires $q_i(x_i, \frac{1}{2}\Delta t)$.
- Taylor expanding plus Cauchy-Kowalewski give

$$\left.\begin{array}{rcl} q_i(x_i,\tau) & = & q_i(x_i,0_+) + \tau\partial_t q(x_i,0_+) \\ & = & q_i(x_i,0_+) + \tau(-\lambda\partial_x q_i(x_i,0_+) + \beta q_i(x_i,0_+)) \; . \end{array}\right\} \tag{81}$$

- In the case considered we have

$$q_i(x_i,0_+) = q_i^n = p_i(x_i) \; , \;\; \partial_x q_i(x_i,0_+) = \Delta_i \; .$$

- The numerical source from (80) is

$$s_i = \beta\left(q_i^n + \frac{1}{2}\Delta t(-\lambda\Delta_i + \beta q_i^n)\right) \; . \tag{82}$$

The ADER scheme for linear advection-reaction

The final form of the ADER scheme is

$$q_i^{n+1} = q_i^n - \frac{\Delta t}{\Delta x}[f_{i+\frac{1}{2}} - f_{i-\frac{1}{2}}] + \Delta t s_i \ , \tag{83}$$

with numerical flux

$$f_{i+\frac{1}{2}} = \begin{cases} \lambda\left(q_i^n + \frac{1}{2}(1-c)\Delta x \Delta_i + \frac{1}{2}r(q_i^n + \frac{1}{2}\Delta x \Delta_i)\right) & , \lambda > 0 \\ \\ \lambda\left(q_{i+1}^n - \frac{1}{2}(1+c)\Delta x \Delta_{i+1} + \frac{1}{2}r(q_{i+1}^n - \frac{1}{2}\Delta x \Delta_{i+1})\right) & , \lambda < 0 \end{cases} \tag{84}$$

and numerical source

$$s_i = \beta\left(q_i^n + \frac{1}{2}\Delta t(-\lambda\Delta_i + \beta q_i^n)\right) \ . \tag{85}$$

In full, for the case $\lambda > 0$, the scheme reads

$$\left.\begin{array}{rcl} q_i^{n+1} & = & q_i^n \quad -c\left[(q_i^n - q_{i-1}^n) + \frac{1}{2}(1-c)\Delta x(\Delta_i - \Delta_{i-1})\right] \\ & & \qquad -cr\left[\frac{1}{4}(q_i^n - q_{i-1}^n) + \frac{1}{2}\Delta x(\Delta_i - \Delta_{i-1})\right] \\ & & \qquad +r\left[(1+\frac{1}{2}r)q_i^n - \frac{1}{2}c\Delta x \Delta_i\right] \ . \end{array}\right\} \tag{86}$$

Remarks on the ADER approach

- Note that if the slopes are all set to zero and we also set to zero the contribution of the source to the numerical flux, then we produce a first-order numerical scheme for the model advection-reaction equation that consists of the first-order upwind method of Godunov for the advection part and an upwind discretisation of the source term, namely

$$q_i^{n+1} = q_i^n - c(q_i^n - q_{i-1}^n) + r\left[\frac{1}{2}cq_{i-1}^n + (1 - \frac{1}{2}c)q_i^n\right] \ . \qquad (87)$$

  This corresponds to one of the schemes analysed in (Roe, 1986) [9] and (Bermudez and Vazquez, 1994) [1] in which the concept of *upwinding the source term* was employed
- By choosing the slopes Δ_i appropriately, we can reproduce the well-known schemes (57), when $\beta = 0$ (no source term)
- The second-order ADER scheme with ENO reconstruction is effectively a blend of the Warming-Beam and the Lax-Wendroff schemes (verify).

- The ADER approach may look complex for constructing a second order method. However for higher order, the steps remain essentially the same
- The ADER approach is capable of producing non-linear schemes of arbitrary order of accuracy in both space and time
- Here we have presented the finite volume version. A discontinuous Galerkin finite element version is also available. See Dumbser et al. (2008) [2]
- An introduction to ADER schemes is found in chapters 19 and 20 of Toro (2009) [12]
- In the last 10 years there have been many developments of the ADER approach due to many researchers. See chapters 19 and 20 of Toro (2009) [12] for references.

Sample numerical results

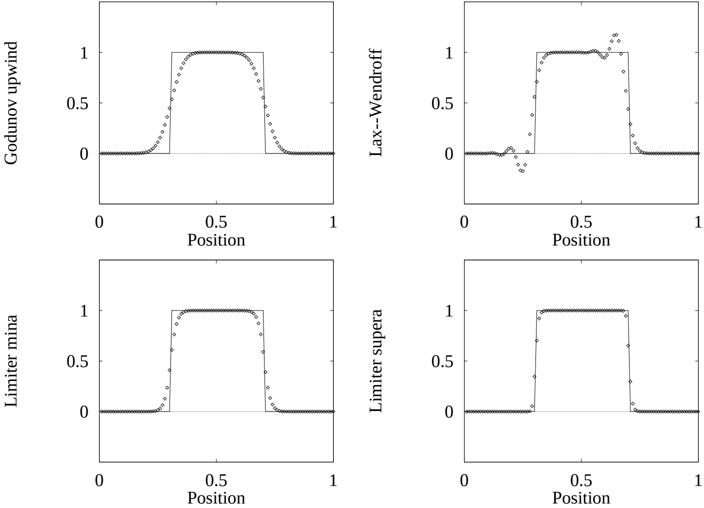

Fig. 8: LAE at $T_{out} = 1$.Top left: Godunov. Top right: Lax-Wendroff
Bottom: WAF method with limiters MINBEE (left) and SUPERBEE (right).

Sample numerical results

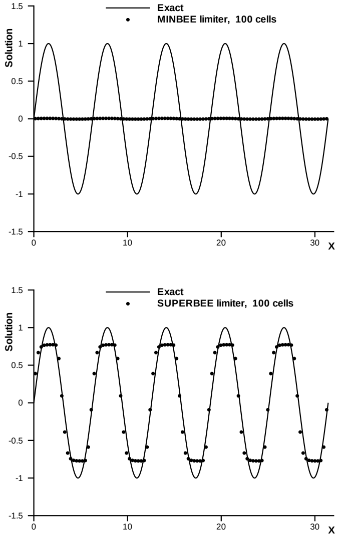

Fig. 9: LAE at $T_{out} = 1000\pi$. Bottom right: ADER 5th order. Rest: Second-order TVD schemes.

Second-Order Schemes for Equation with Source

Consider the model advection-reaction equation

$$\partial_t q + \partial_x f(q) = s(q) \; , \;\; f(q) = \lambda q \; , \;\; s(q) = \beta q \; , \tag{88}$$

where $\lambda > 0$ and $\beta \leq 0$ are two constants. Recall that for the ADER2 method, for $\lambda > 0$ the numerical flux is

$$f_{i+\frac{1}{2}} = \lambda \left(q_i^n + \frac{1}{2}(1-c)\Delta x \Delta_i + \frac{1}{2} r (q_i^n + \frac{1}{2}\Delta x \Delta_i) \right) \; , \tag{89}$$

where

$$c = \frac{\lambda \Delta t}{\Delta x} \, , r = \Delta t \beta \, , \tag{90}$$

are the CFL number and a *reaction number*. The numerical source is

$$s_i = \beta \left((1 + \frac{1}{2} r) q_i^n - \frac{1}{2} c \Delta x \Delta_i \right) \tag{91}$$

and is independent of the sing of λ, positive or negative.

MUSCL-Hancock for source term

To account for the source term, the evolution step to compete the flux reads

$$\left.\begin{array}{rcl}\bar{q}_i^L & = & q_i^L - \frac{1}{2}\frac{\Delta t}{\Delta x}[f(q_i^R) - f(q_i^L)] + \frac{1}{2}\Delta t(\beta q_i^L)\,, \\ \bar{q}_i^R & = & q_i^R - \frac{1}{2}\frac{\Delta t}{\Delta x}[f(q_i^R) - f(q_i^L)] + \frac{1}{2}\Delta t(\beta q_i^R)\,. \end{array}\right\} \quad (92)$$

Compare this to (54). For $\lambda > 0$, simple manipulations give the numerical flux for the MUSCL-Hancock method accounting for the presence of the source as

$$f_{i+\frac{1}{2}} = \lambda\left[q_i^n + \frac{1}{2}(1-c)\Delta x\Delta_i + \frac{1}{2}r(q_i^n + \frac{1}{2}\Delta x\Delta_i)\right]\,. \quad (93)$$

The numerical source for the MUSCL-Hancock method is taken, by construction, to be identical to that of the ADER scheme, namely (91).

The WAF method

The Weighted Average Flux (WAF) method has numerical flux, for the homogeneous linear advection equation, given as

$$f_{i+\frac{1}{2}} = f_{i+\frac{1}{2}}(r,s) = \frac{1}{2}(1+\phi_{i+\frac{1}{2}})(\lambda r) + \frac{1}{2}(1-\phi_{i+\frac{1}{2}})(\lambda s)\,, \qquad (94)$$

where $\phi_{i+\frac{1}{2}}$ is a WAF limiter. To apply WAF to the inhomogeneous case we perform the following steps

- **Evolution of data:** Evolve cell averages q_i^n, q_{i+1}^n to

$$\left.\begin{array}{lllll} \tilde{q}_i^n & = & q_i^n + \frac{1}{2}\Delta t \beta q_i^n & = & (1+\frac{1}{2}r)q_i^n\,, \\ \tilde{q}_{i+1}^n & = & q_{i+1}^n + \frac{1}{2}\Delta t \beta q_{i+1}^n & = & (1+\frac{1}{2}r)q_{i+1}^n\,, \end{array}\right\} \qquad (95)$$

  by solving the ODE

$$\frac{d}{dt}q = s(q)\,, \qquad (96)$$

  by half a time step and initial condition q_i^n and q_{i+1}^n.

- **Riemann problem and flux:** Solve the classical Riemann problem with evolved data $\tilde{q}_i^n$, $\tilde{q}_{i+1}^n$ to compute the usual WAF flux, which now reads

$$f_{i+\frac{1}{2}} = \frac{1}{2}(1+\phi_{i+\frac{1}{2}})(1+\frac{1}{2}r)(\lambda q_i^n)+\frac{1}{2}(1-\phi_{i+\frac{1}{2}})(1+\frac{1}{2}r)(\lambda q_{i+1}^n) \quad (97)$$

- **Numerical source:** Compute the numerical source using the ADER procedure, namely

$$s_i = \beta\left[(1+\frac{1}{2}r)q_i^n - \frac{1}{2}c\Delta x\Delta_i\right] . \quad (98)$$

with WAF slope

$$\Delta_i = \frac{q_{i+\frac{1}{2}} - q_{i-\frac{1}{2}}}{\Delta x} . \quad (99)$$

Here the intercell states are taken as the WAF averaged states

$$\left.\begin{array}{l} q_{i-\frac{1}{2}} = \frac{1}{2}(1+\phi_{i-\frac{1}{2}})q_{i-1}^n + \frac{1}{2}(1-\phi_{i-\frac{1}{2}})q_i^n \ , \\ \\ q_{i+\frac{1}{2}} = \frac{1}{2}(1+\phi_{i+\frac{1}{2}})q_i^n + \frac{1}{2}(1-\phi_{i+\frac{1}{2}})q_{i+1}^n \ . \end{array}\right\} \quad (100)$$

Test problem

We solve the initial-value problem for the linear advection-reaction equation

$$\left.\begin{array}{l} \partial_t q + \lambda \partial_x q = \beta q \quad x \in [-1, 1] \\ \\ q(x, 0) = h(x) = \sin \pi x \end{array}\right\} \tag{101}$$

with periodic boundary conditions, whose exact solution is

$$q(x, t) = h(x - \lambda t) e^{\beta t} \,. \tag{102}$$

M	L_∞-error	L_∞-order	L_1-error	L_1-order
10	$3.28E-2$	xx	-2	
20	$7.86E-3$	2.06	$1.00E-2$	2.08
40	$1.82E-3$	2.11	$2.33E-3$	2.10
80	$4.51E-4$	2.02	$5.74E-4$	2.02

Convergence rates for LAE with source term.
WAF method (non limited). Error measured in two norms, for a sequence of four meshes ($M = 10, 20, 40, 80$).

Exercises

Problem 1: TVD schemes. Show that the following schemes for the linear advection equation (LAE) are TVD: Lax-Friedrichs, FORCE and Godunov upwind (for $\lambda > 0$ and for $\lambda < 0$).

Problem 2: Monotone schemes are TVD. Show that a three-point, monotone scheme for LAE is TVD.

Problem 3: Viscosity form of a scheme. Consider the three-point scheme written in viscous form

$$q_i^{n+1} = q_i^n - \frac{1}{2}c(q_{i+1}^n - q_{i-1}^n) + \frac{1}{2}d(q_{i+1}^n - 2q_i^n + q_{i-1}^n) \tag{103}$$

to solve LAE. By performing a truncation error analysis show that the coefficient of numerical viscosity in the sense of local truncation error is

$$\alpha_{visc} = \frac{1}{2}\Delta x \lambda \left(\frac{d - c^2}{c} \right) . \tag{104}$$

Problem 4: Coefficient of viscosity form of a scheme. Show that by choosing appropriate values of d one can reproduce some well known schemes, that is

$$d(c) = \begin{cases} 1 & \text{Lax-Friedrichs}\,, \\ \frac{1}{2}(1+c^2) & \text{FORCE}\,, \\ |c| & \text{Godunov upwind}\,, \\ c^2 & \text{Lax-Wendroff}\,. \end{cases} \quad (105)$$

Problem 5: Coefficient of viscosity for known schemes. Consider the functions $d(c)$ above.

- Plot all the function $d(c)$ above in the rectangle $[-1, 1] \times [0, 1]$.
- Identify the regions of monotone schemes and of non-monotone schemes.
- Discuss accuracy of the considered schemes in terms of the plot above.

Problem 6: WAF method. Consider the WAF method for LAE with numerical flux

$$f_{i+\frac{1}{2}} = f_{i+\frac{1}{2}}(r,s) = \frac{1}{2}(1+\phi_{i+\frac{1}{2}})(\lambda r) + \frac{1}{2}(1-\phi_{i+\frac{1}{2}})(\lambda s)\,, \qquad (106)$$

where $\phi_{i+\frac{1}{2}}$ is a WAF limiter function.

- Applying the methodology used for deriving flux limiters $\psi(r)$, find the TVD region for WAF and plot it.
- Show that $\psi(r)$ is related to $\phi_{i+\frac{1}{2}}(r)$ via

$$\phi_{i+\frac{1}{2}}(r) = 1-(1-|c|)\psi(r)\,, \qquad (107)$$

where c is the Courant number.

Problem 7: The Kolgan scheme (1972) Kolgan [7] is now recognized to have been the first to propose non-linear schemes. The *linear* version of Kolgan's scheme proceeds as for MUSCL-Hancock but neglecting the data evolution step.

- For LAE show that the numerical flux for the Kolgan scheme is

$$f_{i+\frac{1}{2}} = \begin{cases} \lambda(q_i^n + \frac{1}{2}\Delta x \Delta_i) & \text{if} \quad \lambda > 0\,, \\ \\ \lambda(q_{i+1}^n - \frac{1}{2}\Delta x \Delta_{i+1}) & \text{if} \quad \lambda < 0\,. \end{cases} \tag{108}$$

- For $\lambda > 0$ consider the *linear* version of Kolgan's scheme by taking linear (fixed) slopes

$$\Delta_i = \Delta_{i-\frac{1}{2}} = \frac{q_i^n - q_{i-1}^n}{\Delta x}$$

and write the resulting three-point scheme as

$$q_i^{n+1} = b_{-1} q_{i-1}^n + b_0 q_i^n + b_1 q_{i+1}^n\,, \tag{109}$$

explicitly identifying the coefficients b_{-1}, b_0 and b_1.

- Derive the local truncation error and state the order of accuracy of the scheme.
- Analyse the stability of the scheme using the (a) the von Neumann method, (b) Billett's method and (c) the viscosity form of the scheme.
- Repeat the above with slopes chosen as

$$\Delta_i = \Delta_{i+\frac{1}{2}} = \frac{q_{i+1}^n - q_i^n}{\Delta x} \ .$$

Remark: non-linear Kolgan scheme. The linear version of Kolgan's scheme is *unconditionally unstable*, as shown above. However the non-linear version proposed originally by Kolgan uses a non-linear reconstruction whereby the choice of the slopes is non-linear. In particular Kolgan proposed the use of *minimum slopes*, which is equivalent to choosing the MINMOD slope limiter.

L. Bermúdez and M. E. Vázquez.
Upwind Methods for Hyperbolic Conservation Laws with Source Terms.
Computers and Fluids, 23:1049–1071, 1994.

M. Dumbser, D. Balsara, E. F. Toro, and C. D. Munz.
A Unified Framework for the Construction of One–Step Finite–Volume and Discontinuous Galerkin Schemes.
J. Comput. Phys., 227:8209–8253, 2008.

M. Dumbser and M. Käser.
Arbitrary High Order Non-Oscillatory Finite Volume Schemes on Unstructured Meshes for Linear Hyperbolic Systems.
J. Comput. Phys., 221(2):693–723, 2007.

M. Dumbser, M. Käser, V. A. Titarev, and E. F. Toro.
Quadrature-Free Non-Oscillatory Finite Volume Schemes on Unstructured Meshes for Nonlinear Hyperbolic Systems.
J. Comput. Phys., 226(8):204–243, 2007.

A. Harten and S. Osher.

Uniformly High–Order Accurate Nonoscillatory Schemes I.
SIAM J. Numer. Anal., 24(2):279–309, 1987.

G. S. Jiang and C. W. Shu.
Efficient Implementation of Weighted ENO Schemes.
J. Comp. Phys., 126:202–228, 1996.

V. P. Kolgan.
Application of the Principle of Minimum Derivatives to the Construction of Difference Schemes for Computing Discontinuous Solutions of Gas Dynamics (in Russian).
Uch. Zap. TsaGI, Russia, 3(6):68–77, 1972.

V. P. Kolgan.
Application of the principle of minimising the derivative to the construction of finite-difference schemes for computing discontinuous solutions of gas dynamics.
J. Comp. Phys., 230:2384–2390, 2011.

P. L. Roe.

Upwind Differencing Schemes for Hyperbolic Conservation Laws with Source Terms.
In *Proc. First International Conference on Hyperbolic Problems, Carasso, Raviart and Serre (Editors)*, pages 41–51. Springer, 1986.

P. K. Sweby.
High Resolution Schemes Using Flux Limiters for Hyperbolic Conservation Laws.
SIAM J. Numer. Anal., 21:995–1011, 1984.

E. F. Toro.
A Weighted Average Flux Method for Hyperbolic Conservation Laws.
Proc. Roy. Soc. London, A423:401–418, 1989.

E. F. Toro.
Riemann Solvers and Numerical Methods for Fluid Dynamics. A Practical Introduction. Third Edition.
Springer–Verlag, 2009.

E. F. Toro, R. C. Millington, and L. A. M. Nejad.
Towards Very High–Order Godunov Schemes.

In *Godunov Methods: Theory and Applications. Edited Review, E. F. Toro (Editor)*, pages 905–937. Kluwer Academic/Plenum Publishers, 2001.